right for production of the two species in eq 11 at equal probability, i.e., from a symmetric intermediate or transition state. The fact that mass 48 product is more prominent when initial Fe(II):NO is 1:2 rather than 1:1 reflects the expected greater rate of $H^{15}N^{18}O$ production. The shifting proportions of the three kinds with time is caused by changing relative production rates of the two kinds of HNO. If the intermediate produced by Fe(II) reduction of NO is identical with the species produced in pulse radiolysis, as we believe to be the case for the product of $HN_2O_3^-$ decomposition, it would occur predominantly as NO^- under the conditions of these experiments, since its pK_a is reported to be 4.7.[35]

Registry No. Fe, 7439-89-6; NO_2^-, 14797-65-0; NO, 10102-43-9; $Na_2N_2O_3$, 13826-64-7; N_2O, 10024-97-2; $HN_2O_3^-$, 67180-31-8; HNO, 14332-28-6.

(35) Grätzel, M.; Taniguchi, S.; Henglein, A. *Ber. Bunsenges. Phys. Chem.* **1970**, *74*, 1003.

Contribution from the Department of Chemistry,
State University of New York at Stony Brook, Stony Brook, New York 11794

Aqueous Nitrosyliron(II) Chemistry. 2. Kinetics and Mechanism of Nitric Oxide Reduction. The Dinitrosyl Complex[1,2]

KENNETH A. PEARSALL and FRANCIS T. BONNER*

Received October 26, 1981

The formation constant for $Fe(NO)^{2+}$ is independent of pH in aqueous sulfate (pH 0.5–3.3) and has the value of 0.634 ± 0.023 atm^{-1} at 25.0 °C (I = 2.20 M). At pH 4.6 in the presence of 2.0 M acetate, the constant is 29.0 ± 1.5 atm^{-1} and increases to 70 atm^{-1} at $[OAc^-]$ = 3 M. Acetate ligation is involved in this enhancement, probably one ion per Fe(II) center. With decreasing Fe(II)/NO ratio and above pH 4 the presence of dinitrosyl complex is detected stoichiometrically, with a constant of formation (from $Fe(NO)^{2+}$ + NO) of 0.98 ± 0.15 atm^{-1} (pH 4.6, $[OAc^-]$ = 2.0 M, I = 2.20 M). From kinetic data the value of this constant at pH 6.0 in acetate buffer at I = 3.0 M is inferred to be 15 atm^{-1}, and the probable presence of one OH^- in the Fe(II) coordination sphere is indicated. The reduction of NO by Fe(II) in concentrated acetate buffer at pH 6 is shown to conform to the rate law $-d[Fe(II)]/dt = k_1[Fe(NO)_2^{2+}] + k_2[Fe(NO)_2^{2+}]^2$, where k_1 = (1.6 ± 0.4) × 10^{-4} s^{-1} and k_2 = 0.047 ± 0.002 M^{-1} s^{-1} at 25.0 °C. A dinitrosyl Fe(II) species bearing both formal NO^+ and formal NO^- in a cis relation, and in rapid exchange equilibrium, is postulated, and a possible mechanism for the major (second-order) pathway is discussed.

We have reported that the threshold for reduction of NO by Fe(II) to N_2O occurs at about pH 4, that HNO (or NO^-) is the primary product of this process, and that further reduction to N_2 does not occur below ca. pH 8.[2] The apparent inhibition of electron transfer by H^+ in this case is unusual and reflects remarkable stability on the part of the well-known "brown ring" complex, $Fe(H_2O)_5NO^{2+}$. The complexation equilibrium

$$Fe^{2+} + NO \rightleftharpoons Fe(NO)^{2+} \quad (1)$$

and the redox reaction

$$Fe^{II} + NO + H^+ = Fe^{III} + {}^1/_2N_2O + {}^1/_2H_2O \quad (2)$$

are closely related and broadly relevant to both inorganic and biochemical processes. Nitrosyliron chemistry is important in providing ESR probes, and in other ways, in the study of hemoglobin, cytochrome *c*, and other heme and nonheme proteins.[3,4] Iron is present at the active sites of both nitrite and nitrate reductases;[5,6] it is probable that nitrosyliron chemistry plays a role in microbial denitrification and possibly in nitrification processes as well. Nitrosyliron compounds have been postulated as intermediates in the transformation of inorganic nitrogen in soils.[7]

There are three principal literature reports concerning equilibrium 1. Manchot and Haunschild[8] measured the equilibrium constant by measurement of initial and final pressures of NO brought in contact with a large volume of solution of ferrous ammonium sulfate and reported values of 4.07, 1.58, and 0.661 atm^{-1}, at 0, 18, and 25 °C, respectively, for

$$K_1 = [FeNO^{2+}]/[Fe^{2+}]P_{NO} \quad (3)$$

Abel et al.,[9] using a similar method with $FeSO_4$, reported a value of 0.637 atm^{-1} at 25 °C. Kustin, Taub, and Weinstock[10] reported forward and reverse rate constants for eq 1 to be k_1 = 6.2 × 10^5 M^{-1} s^{-1} and k_{-1} = 1.4 × 10^3 s^{-1} (25 °C); in combination with their own value for NO solubility these data yield K = 0.63 atm^{-1}.

Griffith, Lewis, and Wilkinson[11] characterized the complex $Fe(H_2O)_5NO^{2+}$ as high spin, with magnetic susceptibility showing three unpaired electrons, and described the bonding as NO^+ coordinated to Fe(I). This description was based in part on observation of an NO stretching frequency of 1765 cm^{-1}, near the upper edge of the region 1600–1750 cm^{-1} that

(1) Research supported by the National Science Foundation, Grant No. CHE 78-24176.
(2) Part 1: Bonner, F. T.; Pearsall, K. A. *Inorg. Chem.*, companion paper in this issue.
(3) Gordy, W.; Rexroad, H. N. In "Free Radicals in Biological Systems"; Blois, M. S., Jr., Brown, H. W., Lemmon, R. M., Lindblom, R. O., Weissbluth, M., Eds.; Academic Press: New York, 1961; pp 268–73.
(4) Goodman, B. A.; Raynor, J. B. *J. Chem. Soc. A* **1970**, 2038 and references therein.
(5) Aparicio, P. J.; Knaff, D. B.; Malkin, R. *Arch. Biochem. Biophys.* **1975**, *169*, 102.
(6) Dervartanian, D. V.; Forget, P. *Biochim. Biophys. Acta* **1975**, *379*, 74.
(7) Moraghan, J. T.; Buresh, R. J. *Soil Sci. Am. J.* **1977**, *41*, 47.
(8) Manchot, W.; Haunschild, H. *Z. Anorg. Allg. Chem.* **1924**, *140*, 22.
(9) Abel, E.; Schmid, H.; Pollak, F. *Monatsh. Chem.* **1936**, *69*, 125.
(10) Kustin, K.; Taub, I. A.; Weinstock, E. *Inorg. Chem.* **1966**, *5*, 1079.
(11) Griffith, W. P.; Lewis, J.; Wilkinson, G. *J. Chem. Soc.* **1958**, 3993.

0020-1669/82/1321-1978$01.25/0

has been suggested as indeterminate for discrimination between NO^+ and NO^-.[12] Subsequently, Mosbaek and Poulsen[13] reported the Mössbauer spectrum of solid $[Fe(NH_3)_5NO]Cl_2$ to have the characteristics of a high-spin Fe(III) compound and described the nitrosyl ligand as formal NO^-. In further work they considered the "brown ring" complex and several other compounds, concluding from their Mössbauer spectra that the charge at the iron center is nearly 3+ in all cases, although perhaps intermediate between 2+ and 3+ in aqueous $Fe(H_2O)_5NO^{2+}$.[14] The proposals of Enemark and Feltham[15] regarding six-coordinate $\{MNO\}^n$ groups for $n \geq 7$ suggest that the angle Fe(II)–N–O should be bent (i.e., NO bound as NO or NO^-).

McDonald, Phillips, and Mower[16] have reported an ESR signal ascribable to a dinitrosyl complex in solutions of $FeSO_4$ in contact with NO and in the presence of various anions. The intensity of the signal decreases with increasing acidity and becomes undetectable at pH 4 and below. It increases with increasing basicity to pH 10, and an intensity increase of 2 orders of magnitude occurs between pH 10 and 11. On the basis of their ESR evidence, the authors describe the complex as being mononuclear and containing a single unpaired electron and two equivalent nitrogen nuclei. A further report of ESR evidence for a dinitrosyl complex has been made by Burlamacchi et al.,[17] and related ESR studies of $Fe(H_2O)_5NO^{2+}$ solutions in the presence of sulfide and hydroxide ions have been reported by Goodman and Raynor.[4]

In this paper we report direct chemical evidence for the formation of a dinitrosyliron(II) species when nitric oxide is brought in contact with $FeSO_4$ solution at pH 4 and above and kinetic evidence that this species plays a principal role in the reduction of NO to N_2O by Fe(II). There appear to be no previously reported kinetic studies of this reaction.

Experimental Section

Reagents. Ferrous sulfate, nitric oxide, CO_2, and CF_4 were purified and maintained as described in part 1.[2]

Equilibrium and Kinetics Measurements. All measurements of equilibrium constants and rates were carried out in reaction vessels of the type shown in Figure 1 of part 1 and employed the general procedures described there, including gas chromatographic gas analyses.[2,18] A typical vessel employed in this study had a total volume of 149.7 mL and a sample volume of 3.07 mL; a typical solution volume employed was 20.0 mL. Several reaction vessels of different volumes (ranging as high as 445.6 mL, with sample volume 7.28 mL) and proportions (height/width) were used. As will be reported below, establishment of initial equilibrium between NO and the nitrosyl complexes in solution appeared to be surprisingly slow; the process was facilitated by decreasing the height/width ratio. Phase mixing conditions (as visually assessed) were subject to variation with solution volume and vessel geometry, some combinations giving rise to virtual "resonance" vibrations and attendant pronounced droplet fountain effects inside the cell. As has been stressed previously, laminar flow in the temperature-controlling water jacket is essential for maintenance of an undamped vibration.[19]

Calculations. The partial pressures of individual gases and the total molar quantity of each gas in the reaction vessel were calculated for each sampling time. For NO–CF_4 mixtures, $P^0_{CF_4}$ was determined from the GC analysis of the mixture (sensitivity factors were measured with an uncertainty <1%) and the initial total pressure in the reaction vessel corrected for P_{H_2O}. For subsequent gas samples, P_{CF_4} was reduced each time by the factor $V_g/(V_g + V_{sample})$ (V_g = volume of gas phase in reaction vessel; V_{sample} = sample volume) to allow for CF_4 lost during previous sampling. The partial pressure of a reactant or product gas at time t was calculated from $(P_{CF_4})_t$ and the GC analysis, with corrections for solubility based on Henry's law constants[20] and for previous sampling losses. When CO_2 was used as an internal reference, it was necessary to correct P_{CO_2} for solubility and for HCO_3^- formation, on the basis of the first acid dissociation constant $K_{CO_2H_2O}$, at the particular pH of the experiment.[21]

For calculation of equilibrium constant K_1 (eq 3) under nonreactive conditions (no N_2O formation), we use the relationships

$$n_{FeNO^{2+}} = n^0_{NO} - n_{NO} \quad (4)$$

$$n_{Fe^{2+}} = n^0_{Fe(II)} - n_{FeNO^{2+}} \quad (5)$$

Hence

$$K_1 = \frac{[FeNO^{2+}]}{[Fe^{2+}]P_{NO}} = \frac{n_{FeNO^{2+}}}{n_{Fe^{2+}}P_{NO}} \quad (6)$$

Here n^0_{NO} is the total moles of NO initially added to the reaction vessel, n_{NO} is the total uncomplexed NO present at equilibrium, determined from P_{NO} (gas phase) and Henry's law (solution phase), and $n^0_{Fe(II)}$ is the total initial Fe(II) present in the solution phase. Sample withdrawal was continued until calculations based on successive samples gave concordant results. For reactive conditions, i.e., if the N_2O product is detectable, the additional term $2n_{N_2O}$ is subtracted from each of the expressions (4) and (5), where n_{N_2O} is the total moles of N_2O formed at the time of the measurement.

For kinetic measurements, the concentration of total Fe(II) remaining at time t was calculated from the relation

$$[Fe(II)]_t = [Fe(II)]_0 - 2n_{N_2O}/V_s \quad (7)$$

where V_s is the volume of the solution phase.

General Experimental Conditions and Limitations. As reported in part 1,[2] NO reduction by Fe(II) is substantially faster at pH 6 than at pH 5; in order to investigate kinetics under conditions capable of leading to completion in reasonable time, we chose pH 6, cognizant that above ca. pH 6.5 hydroxide precipitate begins to form. Although our method of following N_2O production does not relate directly to concentrations of individual solution species or to P_{NO} because of the gas solution equilibria that are involved, spectrophotometric methods proved infeasible because of the problem of phase mixing and also because of an observed gradual increase in absorbance over the entire visible range during the later stages of reaction. In other words, the system is on the edge of solution–solid heterogeneity under the conditions chosen. Although phosphate is the usual buffer of choice for pH 6, it could not be used here because of the insolubility of ferrous phosphate, and acetate was therefore used. Since pH 6 is on the edge of acetate's buffer range, high concentrations were required to provide the necessary buffering capacity, with the result that most of the work reported here was done at very high ionic strength (I = 2.20, 3.00 M). This had one advantage in that high acetate concentrations help to keep Fe(II) and Fe(III) in solution under nearly basic conditions. Kinetic experiments with Fe(II) in significant excess over NO could not be carried out by our technique, since 95% or more of the NO initially introduced becomes complexed with Fe, leaving a gas-phase P_{NO} that becomes too low for accurate analysis.

Results

Formation of Mononitrosyl Complex. In the course of our kinetic studies of the redox reaction, we found that more NO was absorbed in the solution phase than could be accounted for by using literature values for the equilibrium constant K_1. It was therefore necessary to measure our own values for K_1 under conditions relevant to our kinetic measurements. First, we tested the method at low pH, avoiding error due to N_2O production. Determinations of K_1 in Na_2SO_4–H_2SO_4 or Na_2SO_4–$NaHSO_4$ buffers, in the pH range 0.5–3.3, are shown

(12) Connelly, N. G. *Inorg. Chim. Acta, Rev.* **1972**, *6*, 82.
(13) Mosbaek, H.; Poulsen, K. G. *J. Chem. Soc. D* **1969**, 479.
(14) Mosbaek, H.; Poulsen, K. G. *Acta Chem. Scand.* **1971**, *25*, 2421.
(15) Enemark, J. H.; Feltham, R. D. *Coord. Chem. Rev.* **1974**, *13*, 339.
(16) McDonald, C. C.; Phillips, W. D.; Mower, H. F. *J. Am. Chem. Soc.* **1965**, *87*, 3319.
(17) Burlamacchi, L.; Marini, G.; Tiezzi, E. *Inorg. Chem.* **1969**, *8*, 2021.
(18) Pearsall, K. A.; Bonner, F. T. *J. Chromatogr.* **1980**, *200*, 224.
(19) Bonner, F. T.; Jordan, S. *Inorg. Chem.* **1973**, *12*, 1363.
(20) (a) Washburn, E. W., Ed. "International Critical Tables"; McGraw-Hill: New York, 1928; Vol. III, pp 256, 259, 276. (b) Stephen, H., Stephen, T., Eds. "Solubilities of Inorganic and Organic Compounds"; Macmillan: New York, 1963; Vol. 1, p 369.
(21) Pearsall, K. A. Ph.D. Dissertation, State University of New York at Stony Brook, Stony Brook, New York, 1981.

Table I. Measurements of K_1 in Sulfate Buffer at 25.0 °C

expt no.	I, M	$n_{Fe(II)}/n_{NO}$	$[Fe(II)]_0$, M	pH	K_1, atm^{-1}
1	2.20	3.13	0.050	0.50	0.651
2	2.20	1.86	0.050	3.3	0.636
3[a]	2.20	1.66	0.050	1.2	0.607
4	2.20	1.57	0.050	0.50	0.607
5	2.20	1.35	0.050	0.50	0.619
6	2.20	1.15	0.050	3.3	0.626
7	2.20	0.84	0.050	0.50	0.668
8	2.20	0.61	0.050	0.50	0.659
					av 0.634 ± 0.023
9	2.20	0.12	0.010	0.50	1.44
10	2.20	0.74	0.010	0.50	0.540
11	0.30	1.80	0.050	1.7	0.790
12	0.30	1.21	0.010	1.6	0.806
13	3.00	3.03	0.050	0.50	0.412

[a] The solution was 0.10 M in total sulfate; the ionic strength was maintained with $NaClO_4$.

Table II. Values of K_1(obsd) in Acetate Buffer[a]

expt no.	$n_{Fe(II)}/n_{NO}$	K_1(obsd), atm^{-1}	expt no.	$n_{Fe(II)}/n_{NO}$	K_1(obsd), atm^{-1}
1	28.8	56.0	4	10.8	29.6
2	16.2	43.3	5	8.7	30.3
3	15.2	38.9	6	4.4	30.3
			7	2.4	28.0
			8	1.8	26.9
			9	1.1	29.3
				av (4–9)	29.0 ± 1.5

[a] Conditions: 25.0 °C; $[Fe(II)]_0$ = 0.050 M; I = 2.20 M; [NaOAc] = 2.00 M; pH 4.60–4.65.

in Table I. Consistency of the values for K_1 at 2.20 M ionic strength demonstrates the reproducibility of the method. The average values 0.634 atm^{-1} at I = 2.20 M and 0.798 atm^{-1} at I = 0.30 M are to be compared with the literature values of 0.637 atm^{-1} for I in the range 0.02–0.15 M (Abel et al.[9]) and 0.63 atm^{-1} for I = 0.50 M (Kustin et al.[10]). K_1 is independent of pH over the range examined (pH 0.50–3.3). It is also independent of total sulfate and individual SO_4^{2-} and HSO_4^- concentrations, since these are present in varying proportions as needed for ionic strength in all cases but experiment 3, in which the overwhelming ion concentration was due to $NaClO_4$. Experiments 9 and 10 illustrate the magnification of error that occurs at low [Fe(II)], due to the small change in gas-phase composition because of NO complexation; however, experiments 11 and 12 do provide concordant results at two different Fe(II) concentration levels.

Observed values K_1(obsd) in acetate buffer measured under very slightly reactive conditions (pH 4.6–4.65) are shown in Table II. The average of the values from experiments 4–9, 29.0 atm^{-1}, is 46 times greater than the measured K_1 in sulfate buffer at the same ionic strength (Table I). It is clear that acetate ion and/or acetic acid have a strong influence on formation of the mononitrosyl complex $FeNO^{2+}$. (Experiments 1–3 (Table II) illustrate an additional limitation of our experimental method. In these cases the partial pressure of NO at equilibrium is very low. Our sample-transfer process involves expansion and liquid-N_2 condensation, and the measurement is subject to vapor-pressure losses since $P_{NO} \approx 0.08$ torr at 77 K. Systematic errors giving the trend in K_1 as shown were observed at $P_{NO} \leq 2$ torr.)

Table III shows observed values K_1(obsd) for different concentrations of acetate ion at three different levels of ionic strength. The experiment at $[OAc^-]$ = 0.0030 M was carried out in 2 M acetic acid, with pH ca. 2.0. Comparison of K_1(obsd) for these conditions with the value observed at $[OAc^-]$ = 0 (sulfate buffer) shows that it is acetate ion, not

Table III. K_1(obsd) (atm^{-1}) at Different Acetate Ion Concentrations and t = 25.0 °C

	K_1(obsd)		
[NaOAc], M	I = 0.30 M[a]	I = 2.20 M[a]	I = 3.00 M[a]
0	0.798 (2)[b]	0.633 (8)	0.412
0.0030		0.755	
0.100	1.32		1.32
1.00			14.3
2.00		29.0 (6)	
2.80			70.2 (2)
2.96			68.1 (3)

[a] $NaClO_4$ used to maintain ionic strengths shown. [b] Number of replicate determinations shown in parentheses.

Table IV. Measurements of K_2 in Acetate Buffer at 25.0 °C[a]

expt no.	pH	$n_{Fe(II)}/n_{NO}$	apparent K_1, atm^{-1}	calcd K_2, atm^{-1}	% Fe(II) as $Fe(NO)_2^{2+}$
1	4.68	0.88	39.4	0.91	3.9
2	4.65	0.64	77.5	0.91	7.5
3	4.31	0.41	−23.2	1.2	17.1
4	4.63	0.38	−22.0	0.91	22.5

[a] Conditions: $[Fe(II)]_0$ = 0.0500 M; [NaOAc] = 2.00 M; I = 2.20 M.

acetic acid, that is responsible for the increase in $[FeNO^{2+}]$ at equilibrium.

The striking effect of acetate ion on the mononitrosyliron(II) formation equilibrium quite clearly involves coordination of OAc^- to Fe(II). It is not a solubility effect: changes in NO solubility that may occur with high acetate concentration were found to be no more than barely within the limits of measurement by our method. Formation of nitrosyl acetate is ruled out because there is no source of NO^+. With the assumption that the mononitrosyl complex includes one or more acetate ions, then the values of K_1(obsd) (Tables II and III) can be expressed as

$$K_1(\text{obsd}) = \frac{[FeNO^{2+}] + [Fe(OAc)_xNO^{(2-x)+}]}{([Fe^{2+}] + [Fe(OAc)_x^{(2-x)+}])P_{NO}} \quad (8)$$

For the case x = 1, with substitution of terms that include K_1 (eq 3)

$$K_{1,OAc} = [Fe(OAc)NO^+]/[FeOAc^+]P_{NO} \quad (9)$$

and

$$K_{OAc} = [FeOAc^+]/[Fe^{2+}][OAc^-] \quad (10)$$

and eq 8 can be rewritten in the form

$$K_1(\text{obsd}) = \frac{K_1 + K_{1,OAc}K_{OAc}[OAc^-]}{1 + K_{OAc}[OAc^-]} \quad (11)$$

If $K_1 << K_{1,OAc}K_{OAc}[OAc^-]$, this relation predicts a linear dependence of $K_1(\text{obsd})^{-1}$ upon $[OAc^-]^{-1}$ if x = 1. The data at I = 3.00 M (Table III) exhibit such a linearity, which may indicate the presence of a single acetate ligand in the principal mononitrosyl complex in acetate solution, although the assumption regarding the magnitude of K_1 is weak at the low-concentration end. The value 3.5 M^{-1} for K_{OAc} in 3 M $NaClO_4$ is available in the literature.[22] In combination with the slope $K_1(\text{obsd})^{-1}$ vs. $[OAc^-]^{-1}$ at I = 3.0 M this yields a value of 3.7 atm^{-1} for $K_{1,OAc}$. However, the combination of 3.5 M^{-1} for K_{OAc} and 0.41 M^{-1} for K_1 (sulfate buffer) does not provide a constant set of calculated values for $K_{1,OAc}$ as based upon eq 11, a circumstance that we believe can be ascribed to uncertainty in the value of K_{OAc}[23] and quite possibly also to

(22) Ciavatta, L.; Nunziata, S. *Ric. Sci.* **1968**, *38*, 109.

significant participation of acetate–iron species of higher degrees of ligation.

Formation of Dinitrosyl Complex. Table II shows the reproducibility of measurements of K_1 in acetate buffer with the molar ratio Fe(II)/NO varying in the range 10.8–1.1. In Table IV we show that apparent K_1 values become variable and even negative when measured under conditions in which $n_{Fe(II)}/n_{NO} < 1$. A negative apparent K_1 indicates that more NO was consumed during equilibration than can be accounted for in terms of mononitrosyliron(II); we assume the formation of a dinitrosyl complex and a constant K_2 defined as[24]

$$K_2 = [Fe(NO)_2^{2+}]/[FeNO^{2+}]P_{NO} \quad (12)$$

With the assumption that the concentration of $Fe(NO)_2^{2+}$ is negligible under the conditions pertaining to Table II, the value of K_1 observed there can be used to calculate K_2. If the terms

$$n_{Fe(II)} = n_{Fe^{2+}} + n_{FeNO^{2+}} + n_{Fe(NO)_2^{2+}} \quad (13)$$

and

$$n^*_{NO} = n_{FeNO^{2+}} + 2n_{Fe(NO)_2^{2+}} \quad (14)$$

are introduced, where n^*_{NO} is the number of moles of NO that cannot be accounted for by analysis of the gas phase, it can be shown that[21]

$$K_2 = \left[\left[\left(\frac{1 + K_1P_{NO}}{K_1P_{NO}}\right)n^*_{NO} - n_{Fe(II)}\right]K_1\right] \Big/ \left[\left[n^*_{NO} - 2\left[\left(\left(\frac{1 + K_1P_{NO}}{K_1P_{NO}}\right)n^*_{NO} - n_{Fe(II)}\right) \Big/ \left(\frac{K_1P_{NO} + 2}{K_1P_{NO}}\right)\right]\right](K_1P_{NO} + 2)\right] \quad (15)$$

The values of K_2 given in Table IV, calculated with use of $K_1 = 29.0$ atm^{-1} (Table II) in eq 15, are in satisfactory agreement with each other. Although the value for experiment 3 appears to be out of line with the others, considerations of error propagation lead us to conclude that the overall error of measurement in K_2 is somewhat greater than 10%.

The average values of K_2 from Table IV can be used to check our assumption that $[Fe(NO)_2^{2+}]$ can be neglected under the conditions of Table II. We calculate that the percentage of Fe(II) present as $Fe(NO)_2^{2+}$ is 0.02% in experiment 4 (Table II) and increases gradually to 2.9% in the case of experiment 9. As seen in Table IV, this percentage increases substantially as the Fe(II)/NO ratio is reduced.

An unsuccessful effort was made to measure K_2 in the presence of sulfate rather than acetate. Initial experimental conditions were designed to establish pH values between 4.5 and 4.75, since dinitrosyl complex is not expected at pH <4. Adequate buffer capacity cannot be achieved with sulfate at pH >4; final pH values were invariably <4, and no evidence of dinitrosyl complex formation was observed. Small quantities of N_2O product were occasionally observed, suggesting that the decline of pH may be caused by occurrence of the redox reaction.

Rate Law for the Fe^{II}–NO Redox Reaction. Table V shows data for a typical kinetic run, and Figure 1 is the corresponding rate plot demonstrating that the reaction is second order in total [Fe(II)]. Although the data in Figure 1 display excellent

Table V. Typical Kinetic Run (Experiment 6, Table VI)[a]

time, min	P_{CF_4}, torr	P_{NO}, torr	$10^5 n_{N_2O}$	$10^3 \times$ [Fe(II)], M
8	198.6	328.4	1.05	9.20
15	195.0	316.9	2.02	8.46
25	191.4	312.7	3.92	7.02
35	187.9	304.2	5.22	6.03
45	184.5	298.1	6.26	5.24
70	181.1	292.7	8.07	3.86
121	177.8	287.1	9.74	2.59
180	174.5	278.1	10.6	1.94

[a] $t = 25.0$ °C; $[Fe(II)]_0 = 0.0100$ M; $n^\circ_{NO} = 3.12 \times 10^{-3}$; $I = 3.00$ M; pH 6.0; $(n_{NO}/n_{Fe(II)})_0 = 11.9$; $V_g/V_s = 6.49$.

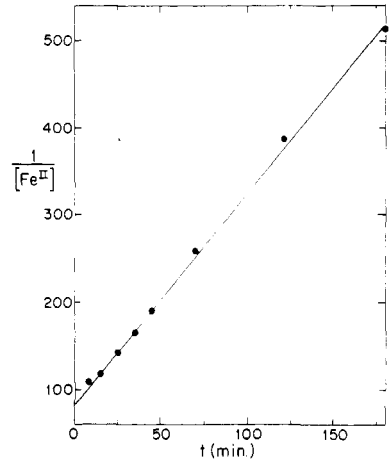

Figure 1. Second-order plot with the data of Table V (experiment 6, Table VI).

linearity up to the point of 78% completion, there is some initial nonlinearity and the intercept occurs somewhat below ($[Fe(II)]_0)^{-1}$ (100 M^{-1}). This indicates that the initial onset of reaction occurs under nonequilibrium conditions. Typically, data points at 15 min were on the line, but in a few cases of less efficient mixing they were not. Experience with equilibrium-constant measurements was similar. Although we cannot offer a detailed explanation, it would appear that the gross mass transfer between phases required to establish initial equilibrium in this complex system occurs more slowly than anticipated. The question must then be raised whether subsequent data points are subject to phase-mixing limitations. Similar methods have been employed in the measurement of exchange processes occurring at half-lives as low as 10 s;[19] mass-transfer limitation in a similar application of mechanical vibration has been reported to occur at times $\tau < 1$ s.[25] In the case of the kinetic data reported here, agitation efficiency depended upon the proportions of the reaction vessel, the volume of solution employed, and adjustments to the vibrator. Rate constants were found to be independent of the magnitude of agitation, over a wide range of visually observable amplitudes. Concordant results were obtained in experiments carried out under similar conditions but in reaction vessels of different proportions and vibration efficiencies and in experiments with different ratios of gas to solution volumes. We are confident that no phase-mixing limitations are reflected in the rate data we report here at times beyond the period of initial equilibration.

Measured values of k_{obsd} in

$$-d[Fe(II)]/dt = k_{obsd}[Fe(II)]^2 \quad (16)$$

are shown in Table VI, where it is seen that k_{obsd} is independent of P^0_{NO} in the mole ratio range NO/Fe(II) = 10–20. Values

(23) The surprisingly greater value 79 M^{-1} has been reported for K_{OAc} in 0.1 M $NaClO_4$: Manku, G. S.; Bhat, A. N.; Jain, B. D. *J. Inorg. Nucl. Chem.* **1969**, *31*, 2533.

(24) In the treatment of K_1 and K_2 from here on the presence of acetate ion is assumed; i.e., by K_1 we mean $K_{1,OAc}$ as defined in eq 9, and the nitrosyl complexes would be more completely represented as $Fe(OAc)NO^+$ and $Fe(OAc)(NO)_2^+$.

(25) Nunes, T. L.; Powell, R. E. *Inorg. Chem.* **1970**, *9*, 1912.

Table VI. Pseudo-Second-Order Rate Constants k_{obsd} (M^{-1} s^{-1}), in $R = k_{obsd}[Fe(II)]^2$, for Mole Ratios NO/Fe(II) ≥ 3[a]

expt no.	$(n_{NO}/n_{Fe(II)})_0$	V_g/V_s	$10^2 k_{obsd}$, M^{-1} s^{-1}
	$[Fe(II)]_0$ = 0.0100 M		
1	19.4	6.49	4.22
2	17.5	6.30	3.92
3	17.4	6.49	4.10
4	17.1	6.46	4.15
5	15.4	6.49	3.90
6	11.9	6.30	4.05
7	11.4	6.48	4.17
8	6.4	6.36	3.00
9	3.0	6.48	1.85
	$[Fe(II)]_0$ = 0.0200 M		
10	19.9	16.4	4.18
11	17.4	17.4	3.70
12	17.2	17.2	3.78
	$[Fe(II)]_0$ = 0.0300 M		
13	13.1	15.5	4.02
14	11.5	15.5	3.83

[a] Conditions: t = 25.0 °C; pH 6.0; I = 3.00 M.

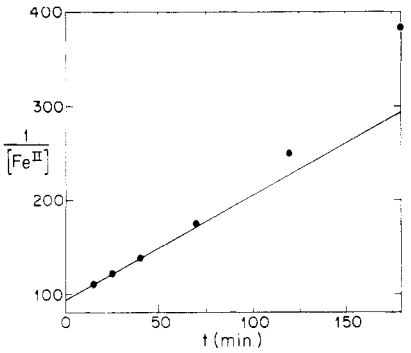

Figure 2. Second-order kinetic plot for experiment 9 (Table VI), $(n_{NO}/n_{Fe(II)})_0$ = 3.0.

determined at $[Fe(II)]_0$ = 0.0200 and 0.0300 M are in agreement with those at 0.0100 M, for which the mean value (experiments 1–7) is equal to 0.0407 ± 0.0012 M^{-1} s^{-1}. Experiments 8 and 9 show that k_{obsd} decreases as the NO/Fe(II) mole ratio decreases below 10. The linearity in the second-order plot for experiment 9 persists for only about 1 half-life and then gives way to upward curvature (Figure 2). Second-order plots for experiments carried out at mole ratios 1.27 (experiment 15) and 1.08 (experiment 16) display continuous upward curvature (Figure 3).

In a reaction system in which no preequilibrium is involved, pseudo-nth-order rate constants would depend upon the concentration of the reactant in large excess. Since k_{obsd} in this case does not vary with P_{NO} in the high mole ratio range, we conclude that the rate law includes the concentration of a species that predominates, i.e., whose concentration varies little with P_{NO}, in this range. The range $(n_{NO}/n_{Fe(II)})_0 < 10$, e.g., in experiments 8 and 9 (Table VI), thus holds the key to determination of the kinetic dependence upon NO. In experiment 9 (Figure 2), P_{NO} can still be taken to be approximately constant over the course of the run, but in experiments 15 and 16 (Figure 3) P_{NO} decreases constantly. The result should be downward curvature in $[Fe(II)]^{-1}$ vs. t if the process remains second order in an Fe(II) species, but upward curvature is observed. We therefore infer that in this region a second pathway has become competitive with the one that predominates at higher ratios and that the new pathway is of kinetic order less than 2 in [Fe(II)].

For the reasons given above, we seek a two-term rate law. First, concerning the high-ratio region in which the process

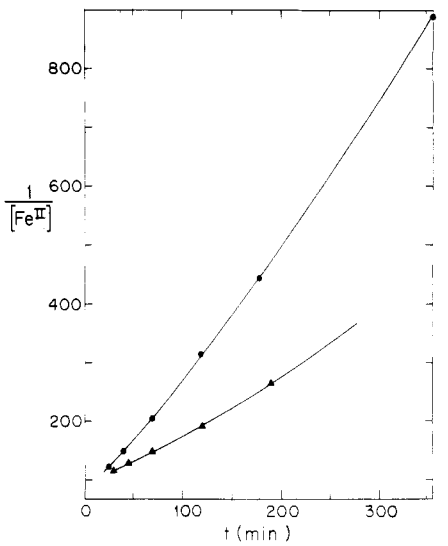

Figure 3. Second-order kinetic plots for two experiments at $[Fe(II)]_0$ = 0.0100, pH 6.0, I = 3.00, and t = 25.0 °C: (●) experiment 15, $(n_{NO}/n_{Fe(II)})_0$ = 1.27; (▲) experiment 16, $(n_{NO}/n_{Fe(II)})_0$ = 1.08.

is unambiguously second order in Fe(II), we consider the possibility that the rate law

$$R = k'[Fe^{2+}]^2 P_{NO} \quad (17)$$

or

$$R = k''[FeNO^{2+}]^2 \quad (18)$$

may apply. These rate laws were integrated[21] and rate constants k' and k'' computed for experiments 1–9 (Table VI), with an appropriate value of K_1 (Table III) but with neglect of dinitrosyl complex formation, as an approximation. All rate plots were linear for NO/Fe(II) ratios above 3 (experiments 1–8), but both rate laws showed a dependence of rate constant upon mole ratio similar to that observed for analytical Fe(II) (Table VI). These rate laws assume first- and second-order dependence upon P_{NO}, respectively; neither assumption matches the data.

Since we have demonstrated that the onset of Fe^{II}–NO redox reactivity occurs at pH ca. 4[2] and the ESR signal that has been ascribed to a dinitrosyl complex is similarly observed only at pH 4 and above,[16] it seems highly probable that the reactive species is $Fe(NO)_2^{2+}$. We therefore consider the possibility that the high-ratio term in the rate law is

$$R = k_2[Fe(NO)_2^{2+}]^2 \quad (19)$$

which can be written in integrated form[21] as

$$\frac{1 + K_1 P_{NO} + K_1 K_2 P_{NO}^2}{K_1 K_2 [Fe(II)] P_{NO}^2} = k_2 t + \text{constant} \quad (20)$$

This rate law cannot be subjected to direct experimental test without a value for K_2 that is valid under the conditions of the kinetic runs. In particular, K_2 has been measured at pH 4.3–4.7 (Table IV); the evidence indicates that the constant is pH dependent but it cannot be measured at pH 6.0 due to intervention of the redox reaction itself. The data of experiments 1–9 (Table VI) have been treated in terms of eq 20 at a series of trial values of K_2, with the results shown in Table VII. Linear kinetic plots were observed for all values of K_2 and for all mole ratios 6.4 and above. The closest match for all mole ratios is given by the trial value K_2 = 15 atm^{-1}; the standard deviation for this column is 4.7% of the mean value, compared with 16% on the left (K_2 = 7.6) and 8.4% on the right (K_2 = 23). More important, the two runs whose values of k_{obsd} show a decrease with decreasing mole ratio (experi-

Table VII. Rate Constants k_2, in $R = k_2[Fe(NO)_2^{2+}]$, Calculated on the Basis of Eq 20 Applied to the Data of Experiments 1–9 (Table VI), at Different Trial Values of K_2 (atm^{-1})

expt no.	$(n_{NO}/n_{Fe(II)})_0$	k_2, M^{-1} s^{-1}: K_2 = 0.76	K_2 = 7.6	K_2 = 15	K_2 = 23
1	19.4	0.142	0.0522	0.0472	0.0455
3	17.4	0.153	0.0522	0.0467	0.0477
4	17.1	0.154	0.0525	0.0468	0.0450
5	15.4	0.160	0.0510	0.0450	0.0430
7	11.4	0.227	0.0602	0.0508	0.0478
8	6.4	0.310	0.0580	0.0440	0.0393
9	3.0	0.593	0.0768	0.0482	0.0387

Table VIII. Experimental First-Order Rate Constants k_1 and k_1', Determined According to Eq 22 and 23[a]

expt no.	V_g/V_s	$(n_{NO}/n_{Fe(II)})_0$	$10^5k_1'$, s^{-1}	10^5k_1, s^{-1}
15	2.62	1.27	18.3[b]	28.3[b]
16	4.72	1.08	9.17	14.2
17	4.72	0.57	7.00	13.7
18	1.87	0.44	10.3	21.5
19	1.87	0.27	8.83	15.3

[a] Conditions: pH 6.0; I = 3.00 M; $[Fe(II)]_0$ = 0.0100 M; t = 25.0 °C. [b] Initial slopes of nonlinear plots.

ments 8 and 9, Table VI) show k_2 values within 1 standard deviation of the mean in this column, compared with a trend above the mean at K_2 = 7.6 atm^{-1} and an opposite trend at K_2 = 23 atm^{-1}.

The value K_2 = 15 atm^{-1} appears to be a good approximation under the conditions of the experiment (pH 6.0, [NaOAc] = 2.96 M, I = 3.00 M). It is greater than K_2 at lower pH, yet smaller than K_1, as expected. We do not believe the match to be fortuitous, and to demonstrate that other rate laws cannot also be caused to conform to our data by adjustment of K_2, we examined the second-order rate law in $[FeNO^{2+}]$ (eq 18) taking $Fe(NO)_2^{2+}$ formation into account, for which case

$$\frac{1 + K_1P_{NO} + K_1K_2P_{NO}^2}{[Fe(II)]K_1P_{NO}} = k_2't + \text{constant} \quad (21)$$

We were unable to find a value of K_2 that gave a satisfactorily constant set of rate constants k_2' for experiments 1–9 and conclude on empirical grounds that none can be found.

The behavior of experiment 9, when plotted according to the rate law of eq 19, is similar to that displayed in Figure 2; i.e., it is linear over a substantial period and then gradually rises. Data for kinetic runs in the low-mole-ratio region plotted in the same way show continuous curvature. However, when these data are treated according to either of the first-order rate laws

$$R = k_1[Fe(NO)_2^{2+}] \quad (22)$$

$$R = k_1'[FeNO^{2+}] \quad (23)$$

in which cases

$$\ln\left(\frac{K_1K_2P_{NO}^2[Fe(II)]}{1 + K_1P_{NO} + K_1K_2P_{NO}^2}\right) = k_1t + \text{constant} \quad (24)$$

and

$$\ln\left(\frac{K_1P_{NO}[Fe(II)]}{1 + K_1P_{NO} + K_1K_2P_{NO}^2}\right) = k_1't + \text{constant} \quad (25)$$

linear plots are obtained (e.g., Figure 4) with the exception of experiment 15 (Figure 5), which appears to be a borderline case. First-order rate constants for this series, based on the

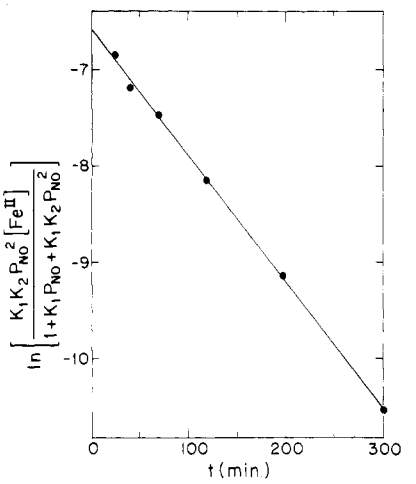

Figure 4. Kinetic plot of data for experiment 18, according to the rate law $R = k_1[Fe(NO)_2^{2+}]$: $[Fe(II)]_0$ = 0.0100 M; pH 6.0; I = 3.00 M; t = 25.0 °C; $(n_{NO}/n_{Fe(II)})_0$ = 0.44.

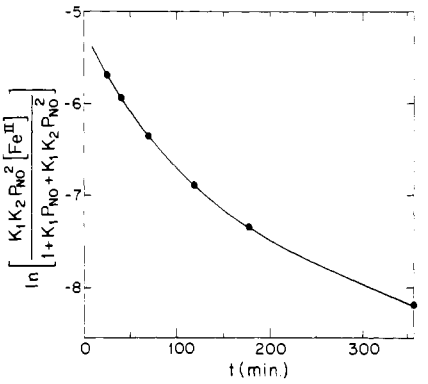

Figure 5. Kinetic plot of data for experiment 15, according to the rate law $R = k_1[Fe(NO)_2^{2+}]$: $[Fe(II)]_0$ = 0.0100 M; pH 6.0; I = 3.00 M; t = 25.0 °C; $(n_{NO}/n_{Fe(II)})_0$ = 1.27.

value K_2 = 15 atm^{-1}, are shown in Table VIII. Scatter in the values for experiments 16–19 is substantial in both cases, and there appears to be no kinetic basis for distinguishing between rate laws 22 and 23 without going to the lower NO/Fe(II) ratios that are not accessible to our method. However, there is a compelling chemical reason for choosing rate law 22 over 23, and that is that if there is a mononitrosyliron(II)-dependent pathway, then the redox reaction should occur at pH <4, but it does not. We therefore opt for a pathway dependent upon dinitrosyl complex.

The two-term rate law that emerges from our data is therefore

$$-\frac{d[Fe(II)]}{dt} = k_1[Fe(NO)_2^{2+}] + k_2[Fe(NO)_2^{2+}]^2 \quad (26)$$

where $k_1 = (1.6 \pm 0.4) \times 10^{-4}$ s^{-1} (Table VIII) and k_2 = 0.0470 ± 0.0022 M^{-1} s^{-1} (Table VII). To test the validity of this rate law, we apply it in the integrated form[26]

$$\ln\left(k_1\frac{1 + K_1P_{NO} + K_1K_2P_{NO}^2}{K_1K_2P_{NO}^2[Fe(II)]} + 2k_2\right) = k_1t \quad (27)$$

to borderline cases in which neither pathway predominates. Experiment 9, at NO/Fe(II) = 3.0, does not conform well to second-order behavior (Figure 2), and experiment 15, at NO/Fe(II) = 1.27, does not conform to first-order behavior

(26) Capellos, C.; Bielski, B. H. J. "Kinetic Systems: Mathematical Description of Chemical Kinetics in Solution"; Wiley-Interscience: New York, 1972; pp 85–7.

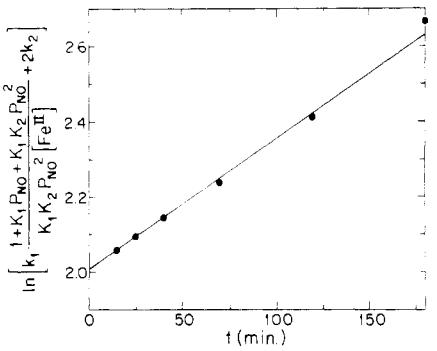

Figure 6. Data of experiment 9 (Figure 2) plotted according to the two-term rate law eq 26.

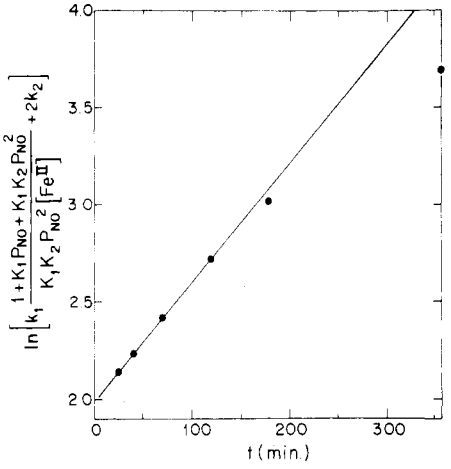

Figure 7. Data of experiment 15 (Figure 5) plotted according to the two-term rate law eq 26.

(Figure 5). Data for both experiments are replotted according to eq 27 in Figures 6 and 7. Although the fit is not perfect, it can be seen that there is a striking improvement upon Figures 2 and 5 and that the two-term rate law models the behavior of this system very well.

Discussion

The effect of acetate, in enhancing the capacity of Fe(II) to form mononitrosyl complex, can be understood in terms of bonding. Reduced nitroprusside, $Fe(CN)_5NO^{3-}$, has been described as NO bonded to Fe(II),[27] and the trans-CN^- group has been shown to be labile due to a trans effect of the nitrosyl group.[28] In the strong ligand field of CN^- the orbital energy levels are reordered with respect to those in $Fe(H_2O)_5NO^{2+}$, with a consequent change in the extended π system over which the odd electron of NO may be stabilized. The ligand field of CH_3COO^- may exert a similar stabilizing influence upon replacing H_2O in the Fe(II) coordination sphere; the partial π character of the carbonyl group should assist delocalization of the odd electron. It is not known whether acetate is mono- or bidentate in this complex, but bidentate bonding should enhance the stabilizing effect.

It seems probable that the dinitrosyl complex identified in this study is either identical with or bears a close relation to the species that have been observed by ESR. We find a threshold for NO reduction at pH 4 and a major kinetic pathway that depends upon the dinitrosyl complex. The formation constant for the dinitrosyl complex, in turn, is clearly pH dependent. McDonald et al.[16] report an ESR signal in neutral NO–$FeSO_4$ solutions whose intensity falls off with decreasing pH and becomes undetectable below pH 4. It is at pH 11 that hyperfine structure indicates the involvement of two NO groups and suggests OH^- complexation as well. In the presence of phosphate, however, a much more intense signal was observed in neutral solution, which was also unobservable at pH <4, that depended on pH and exhibited hyperfine components, indicating two equivalent N nuclei and two equivalent P nuclei. Strong ESR spectra were reported by McDonald et al. for neutral aqueous solutions of Fe(II) treated with NO in the presence of several other anions, and weaker spectra were reported for solutions in the presence of four anions, one of which is acetate. The acetate case is described as giving rise to "complex, poorly resolved, hyperfine structure". Burlamacchi et al.[17] also report the presence of a pH 4 threshold and describe the ESR spectra of a number of species that are reported to be dinitrosyl halide complexes. Goodman and Raynor[4] could not detect an ESR signal in the case of neutral $FeSO_4$ treated with NO until sulfide was added, but it seems possible that their initially "neutral" solution was at pH <4; we have observed that commercial $FeSO_4$ preparations yield acidic aqueous solutions.

By analogy to the known structure of the red Roussin's salt $[Fe(NO)_2SEt]_2$, McDonald et al. proposed that Fe(II), NO, and anions A (e.g., OH^-, HPO_4^{2-}, etc.) form an equilibrium system between a tetrahedral, paramagnetic monomer and its corresponding diamagnetic dimer:

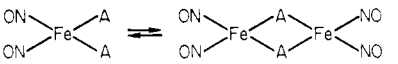

(28)

Similar tetrahedral structures were proposed to account for the ESR observations of Burlamacchi et al.[17] on Fe(II)–NO–halide systems, but Goodman and Raynor[4] considered octahedral coordination much more probable in their studies of Fe^{II}–NO in the presence of sulfide and dithionite.

Anions of the kind $Fe(NO)_2X_2^-$ (X = Cl^-, Br^-, I^-) have been prepared and well characterized by Connelly and Gardner,[29] and Gwost and Caulton have described the formation of such complexes by reductive nitrosylation.[30] There seems no reason to doubt the possibility that tetrahedral dinitrosyl structures of the kind proposed by McDonald et al.[16] and Burlamacchi et al.[17] give rise to the observed ESR signals. Unlike the cases discussed in ref 29 and 30, however, in which identifiable redox processes take place, each of the species presented as paramagnetic in ref 16 and 17 must include an added electron in order to be paramagnetic, and the origin of this electron is nowhere discussed. The necessary end cannot be achieved simply by internal rearrangements in which Fe(II), NO, and robust anions are the starting materials. It is difficult to visualize a redox step as part of the preequilibrium process that precedes our observation of release of the "real" (i.e., stoichiometric) reduction product, N_2O. In addition, the relation between the two complexes appears in our work to be close. The mononitrosyl complex is certainly octahedral, and it seems unlikely that formation of the dinitrosyl would require the drastic change in coordination geometry on the part of its precursor that would be involved in going tetrahedral.

For the above reasons we doubt that the kind of dinitrosyl species described by McDonald et al.[16] is the active reactant in the NO reduction process examined here. We consider octahedral coordination and take note of the fact that acetate is present as a ligand. This is reminiscent of the significant role of anions associated with the ESR signals;[16,17] while our evidence suggests bonding of one acetate ligand, the possibility of a diacetato complex is not precluded. The evident pH dependence of dinitrosyl complex concentration (and ESR signal intensity) leads us to postulate that OH^- is present as

(27) McCleverty, J. A. *Chem. Rev.* **1979**, *79*, 64.
(28) Cheney, R. P.; Simic, M. G.; Hoffman, M. Z.; Taub, I. A.; Asmus, K.-D. *Inorg. Chem.* **1977**, *16*, 2187.
(29) Connelly, N. G.; Gardner, C. *J. Chem. Soc., Dalton Trans.* **1976**, 1525.
(30) Gwost, D.; Caulton, K. G. *Inorg. Chem.* **1973**, *12*, 2095.

a ligand and plays a key role in formation of the dinitrosyl complex. This implies acidity on the part of a species such as $Fe(OAc)(NO)(H_2O)_4^+$ that in some way provides a route and position for addition and stabilization of a second nitrosyl group. This is consistent with the report of McDonald et al.[16] that $FeSO_4$ solutions become more acidic during treatment with NO and with our own experience of being unable to hold such solutions, unbuffered, at pH >4. From our two values for K_2 (1.0 atm^{-1} at pH 4.65, 15 atm^{-1} at pH 6) we consider it likely (but not proven) that the complex includes a single OH^- ion. While processes involving hydroxide attack at nitrosyl can be imagined, e.g., that shown by eq 29, this is

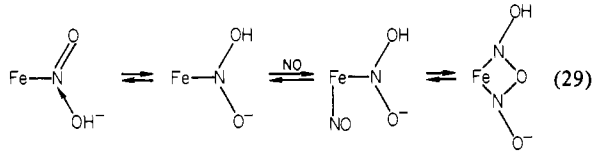

(29)

unlikely because they would promote oxygen exchange between NO and solvent H_2O. In tracer experiments with Fe(II), $HN_2O_3^-$, and $^{15}N^{18}O$ no dilution of mass 47 relative to mass 45 in product N_2O was observed, as would be expected if exchange were to occur.[2]

The major pathway in the Fe(II)–NO reaction involves interaction between dinitrosyls and must produce HNO or NO^-,[2] so that formation of the N–N bond in product N_2O is not concerted.[31] One complex must therefore effectively reduce a nitrosyl ligand of the other, in a process that cannot occur between mononitrosyls. These restrictions quickly eliminate most reasonable mechanistic schemes. We postulate that the dinitrosyl complex is octahedral, of essentially Fe(II) character, bearing cis nitrosyls, one of which is linear and the other bent (i.e., formally NO^+ and NO^-). A precedent for such a structure is provided one row below Fe, by the example of $[RuCl(NO)_2(PPh_3)_2]^+$.[32] In this case the two nitrosyl types have been shown to undergo exchange equilibration[33] on a time scale that may be rapid enough to account for the ESR observation of equivalent nitrosyl nitrogens.[16] The NO^+ nitrogen would be subject to nucleophilic attack, while the other can be considered, in a sense, prereduced. If the oxygen of a nitrosyl ligand can possess significant nucleophilicity, as would be implicit in a resonance structure such as

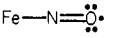

then a process such as the following could occur:

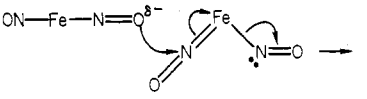

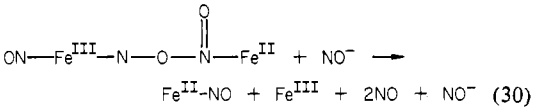

(30)

(The formulation of the dinitrosyl complex as containing nonequivalent NO groups is not strictly essential, since entry of the reacting group could of itself cause a differentiation.) This proposal suffers the weakness that other nucleophiles, notably acetate, would presumably participate yet do not appear to do so. However, it correlates well with the observed change of mechanistic pathway at low dinitrosyliron(II) concentration.

With regard to the first-order, low-stoichiometric-ratio pathway, very little can be said. Our data do not distinguish kinetically between the mono- and dinitrosyl complexes as reactive species, although the latter is the clear choice on chemical grounds. However, it is possible that the process is third-order in NO, e.g., involving an interaction

$$Fe(NO)_2^{2+} + NO \rightarrow \text{products} \qquad (31)$$

and this case has not been tested. It is not out of the question, however, that a partially reduced (formal NO^-) ligand could become fully reduced by a process initiated elsewhere within the same complex.

Acknowledgment. We wish to thank Professors Joseph W. Lauher and Stephen A. Koch for helpful discussions.

Registry No. Fe, 7439-89-6; NO, 10102-43-9.

(31) There is some apparent ambiguity about this conclusion, since the $^{15}N^{18}O$ tracer experiments reported in part 1 were carried out under conditions in which the first-order pathway is (1) predominant and (2) borderline but significant, i.e., with NO/Fe(II) mole ratios 1.0 and 2.0, respectively. The isotopic evidence shows that the degree of scavenging of HNO by $H^{15}N^{18}O$ is greater in case 2 than case 1, however, clearly indicating nonconcerted N_2O production in the second-order process.

(32) Pierpont, C. G.; Eisenberg, R. *Inorg. Chem.* **1972**, *11*, 1088.

(33) Collman, J. P.; Farnham, P.; Dolcetti, G. *J. Am. Chem. Soc.* **1971**, *93*, 1788.